



Fuzzy cluster analysis of high-field functional MRI data[☆]

Christian Windischberger^a, Markus Barth^b, Claus Lamm^c,
Lee Schroeder^d, Herbert Bauer^c, Ruben C. Gur^d, Ewald Moser^{a,b,d,*}

^a*NMR Group, Institute for Medical Physics, University of Vienna, Währingerstrasse 13, A-1090 Vienna, Austria*

^b*Department of Radiodiagnostics, University and General Hospital Vienna,
Währinger Gürtel 18-20, A-1090 Vienna, Austria*

^c*Brain Research Laboratory, Institute of Psychology, University of Vienna, Liebiggasse
5, A-1090 Vienna, Austria*

^d*Brain Behavior Laboratory, Department of Psychiatry, University Pennsylvania Medical Center,
Gates Building, Philadelphia, PA 19104, USA*

Received 21 December 2000; received in revised form 8 June 2001; accepted 13 June 2001

Abstract

Functional magnetic resonance imaging (fMRI) based on blood–oxygen level dependent (BOLD) contrast today is an established brain research method and quickly gains acceptance for complementary clinical diagnosis. However, neither the basic mechanisms like coupling between neuronal activation and haemodynamic response are known exactly, nor can the various artifacts be predicted or controlled. Thus, modeling functional signal changes is non-trivial and exploratory data analysis (EDA) may be rather useful. In particular, identification and separation of artifacts as well as quantification of expected, i.e. stimulus correlated, and novel information on brain activity is important for both, new insights in neuroscience and future developments in functional MRI of the human brain. After an introduction on fuzzy clustering and very high-field fMRI we present several examples where fuzzy cluster analysis (FCA) of fMRI time series helps to identify and locally separate various artifacts. We also present and discuss applications and limitations of fuzzy cluster analysis in very high-field functional MRI: differentiate temporal patterns in MRI using (a) a test object with static and dynamic parts, (b) artifacts due to gross head motion artifacts. Using a synthetic fMRI data set we quantitatively examine the influences of relevant FCA parameters on clustering results in terms of receiver–operator characteristics (ROC) and compare them with a commonly used model-based correlation analysis (CA) approach. The application of FCA in analyzing *in vivo* fMRI data is shown for (a) a motor paradigm, (b) data from multi-echo imaging, and (c) a fMRI study using

[☆] This is an extended and revised version of C. Windischberger, E. Moser, M. Barth, Fuzzy cluster analysis of functional MRI data, in: K.-P. Adlassnig (Ed.), *Fuzzy Diagnostic and Therapeutic Decision Support*, Österreichische Computer Gesellschaft, Vienna, Austria, 2000, pp. 111–118.

* Corresponding author. Tel.: +43-1-4277-60713; fax: +43-1-4277-9607.

E-mail address: ewald.moser@univie.ac.at (E. Moser).

mental rotation of three-dimensional cubes. We found that differentiation of true “neural” from false “vascular” activation is possible based on echo time dependence and specific activation levels, as well as based on their signal time-course. Exploratory data analysis methods in general and fuzzy cluster analysis in particular may help to identify artifacts and add novel and unexpected information valuable for interpretation, classification and characterization of functional MRI data which can be used to design new data acquisition schemes, stimulus presentations, neuro(physio)logical paradigms, as well as to improve quantitative biophysical models.

© 2002 Elsevier B.V. All rights reserved.

Keywords: Fuzzy logic; Clustering; Functional MRI; BOLD; High magnetic field

1. Introduction

Compared to other in vivo brain mapping modalities like positron emission tomography (PET), single photon emission computed tomography (SPECT), electro-encephalography (EEG), magneto-encephalography (MEG), or near-infrared spectroscopy (NIRS), functional magnetic resonance imaging (fMRI) uniquely combines the acquisition of both anatomical and functional information with the best combination of spatial and temporal resolution currently available. However, as fMRI measures the haemodynamic responses to neuronal stimuli rather than the actual neuronal activation, special procedures during data acquisition and post-processing are required to ensure that fMRI activation maps show activation as close as possible to the site of neurons being activated during stimulus presentation. High signal changes in draining veins distant from the site of neuronal activity or stimulus correlated head motions may mask neuronal activation and, therefore, have to be identified and separated. Apart from the proper choice of acquisition parameters, as well as MR scanner performance, image analysis is, thus, a major issue in fMRI.

Most fMRI studies so far have been performed at 1.5 T field strength. Signal-to-noise ratio (SNR), at first glance, seems sufficient for a whole range of brain mapping studies based on the BOLD-effect [28]. Nonetheless, the original work was performed on rat brain at 7 T [35] and at 4 T in human brain [36]. Mainly the wide spread availability of clinical scanners operating at 1.5 T has driven fMRI research. Recently, very high-field (i.e. $B_0 = 3$ T) fMRI has been introduced and has shown several advantages over standard fMRI at 1.5 T, including higher SNR, functional contrast and increased specificity towards microvasculature [19,41,49,50].

In a typical fMRI session, a number of slices is acquired repetitively, i.e. up to thousand times, while a stimulus paradigm is applied (e.g. finger tapping in a simple motor study). These (often huge) data sets are analyzed in a pixel-by-pixel fashion, using either model-based statistical methods or data-driven, exploratory approaches (exploratory data analysis (EDA)). The first group of methods includes univariate [3] or multivariate techniques, like (rotated) principal component analysis (PCA) [2,48], as well as techniques based on the general linear model [17,18]. As the major part of the analysis, the time-course of every pixel is compared to a predefined model of the expected haemodynamic response. Most often, this model function is derived by convolving the stimulus paradigm with a “typical” haemodynamic response function. Furthermore, unrealistic assumptions about noise

distribution in time and space are made, leading to partly invalid or inefficient statistical tests [39,40].

Maybe the most serious problem is caused by physiological noise (i.e. signal fluctuations due to respiration and cardiac action), more or less unrelated to the paradigm and strongly influenced by the details of the data sampling method applied [12–30,33]. In order to reduce problems resulting from unknown noise sources, statistical approaches like statistical parametric mapping (SPM¹) rely on heavy smoothing of the data, which certainly affects both, sensitivity and specificity of the fMRI methods. Smoothing seems particularly inappropriate in fMRI research as it may degrade the inherently good spatial resolution. A more detailed discussion may be found in Raz and Turetzky [40]. These authors, similar to others [1,42,54], use wavelet shrinkage methods and combine it with established statistical procedures in order to relax the unrealistic assumptions on the noise distributions. Purely data driven approaches do not require exact knowledge of the stimulation paradigm or the noise distribution, they rather search for various “interesting” time-courses. Among the methods in this group are hierarchical k-means clustering [15,23], fuzzy C-means clustering [7,9,21,30,31,43], or neural network techniques [16,34]. These techniques can increase reproducibility and specificity of fMRI results [5,7,31]. This approach will gain even more power in combination with very high-field fMRI as SNR is increasing and scanner noise may be separated from physiologic noise and paradigm-related signal changes more easily.

In our data-driven, exploratory analysis approach, we apply a fuzzy cluster analysis (FCA) technique [9,27,43,45], that takes advantage of fuzzy logic algorithms to enhance clustering performance and to improve fMRI results. This “fuzziness”, of course, does not reduce the significance of the final results but helps separating voxel time-courses on a finer scale (i.e. all membership values between 0 and 1 are acceptable). “Crisp” clustering accepts 0 or 1 only, which is not particularly appropriate in biological systems.

In this paper, we describe the basic fuzzy cluster procedure applied as well as details of the actual preprocessing performed. After a short description of fMRI methods used we will demonstrate the potential of FCA to differentiate temporal patterns in MRI using a test object with static and dynamic parts. Examples will be given on how FCA helps to recognize artifacts due to gross head motion artifacts. Using a synthetic fMRI data set [2] we will quantitatively examine the influences of relevant FCA parameters on clustering results in terms of receiver–operator characteristics (ROC) and compare them with a commonly used model-based correlation analysis (CA) approach. Additionally, the performance of FCA in analyzing *in vivo* fMRI data from a motor paradigm will be shown and compared quantitatively to CA. Data from multi-echo imaging experiments provide additional information by utilizing information from the echo time dependence of the fMRI signal. We demonstrate how to integrate this “fifth” dimension (in addition to three spatial and one temporal) into time series analysis and how an exploratory method like FCA can be used to gain further biophysical information by classification of activated areas based on the underlying vascular sources [4,5]. Finally, results from a fMRI study using cognitive stimuli will emphasize the potential of FCA in exploring fMRI data to find initially unexpected information.

¹ <http://www.fil.ion.ac.uk/spm>.

2. Materials and methods

2.1. Cluster analysis

The most important feature of all EDA methods is that they are data-driven and, thus, in principle bias- and model-free. The first clustering approach of brain fMRI data was a “hard” or “crisp” k-means (temporal) clustering proposed by Ding et al. [14]. It was further described and compared with hierarchical clustering by Goutte et al. [23], and a hybrid of hierarchical and k-means clustering was first applied to fMRI by Filzmoser et al. [15]. A fuzzy C-means variant was introduced by Scarth et al. [43], which has the advantage over the hard (crisp) variant that it is less prone to converge to a local minimum too early [46]. This method was implemented in the software package EvIdentTM (EVENT IDENTification) developed at the Institute of Biomedicine (NRC, Winnipeg, Canada).² For all FCA results shown in this paper EvIdentTM, Version 5.2 was used.

Consider N voxels with P time points each and a fixed number of C clusters. The following function [11] is minimized during the procedure (a modified version is used in EvIdentTM):

$$J_m = \sum_{k=1}^N \sum_{i=1}^C (\mu_{ik})^m d_{ik}^2 \quad (1)$$

μ_{ik} is the $n \times c$ matrix of fuzzy membership functions, m is the factor which controls the “fuzziness”. The variable d_{ik} can be any distance metric, i.e. the distance between the k th time-course $\mathbf{x}_k = [x_{k1}, x_{k2}, \dots, x_{kP}]^T$ and the i th cluster centroid $\mathbf{v}_i = [v_{i1}, v_{i2}, \dots, v_{iP}]^T$.

$$d_{ik}^2 = \|\mathbf{x}_k - \mathbf{v}_i\|_A^2 = (\mathbf{x}_k - \mathbf{v}_i)^T \mathbf{A} (\mathbf{x}_k - \mathbf{v}_i) \quad (2)$$

Matrix \mathbf{A} is a positive definite ($P \times P$) matrix chosen to optimize the shape of the clusters. Here, \mathbf{A} is chosen to be the identity matrix so that Euclidean distance is used and hyperspherical clusters are formed [45]. After cluster centers are initialized using either maximum dispersion or random distribution [46], the cluster membership map μ_{ik} is calculated for each cluster i from the relationship

$$\mu_{ik} = \frac{1}{\sum_{j=1}^C (d_{ik}/d_{jk})^{2/(m-1)}}; \quad \forall 1 \leq i \leq C, 1 \leq k \leq N \quad (3)$$

for each voxel k and for the fuzzy index m . After the calculation of all cluster membership maps, in a second step, the centroids v_{ij} are updated:

$$v_{ij} = \frac{\sum_{k=1}^N (\mu_{ik})^m x_{kj}}{\sum_{k=1}^N (\mu_{ik})^m}; \quad \forall 1 \leq i \leq C, 1 \leq j \leq P \quad (4)$$

Clustering is performed via this two-stage iterative process [46] and is repeated until intra-cluster distances are minimized and inter-cluster distances are maximized, or a predefined number of iterations (maximum 50) has been reached. To speed up computation

² <http://www.ibd.nrc.ca/informatics/evident.html>.

and to improve specificity of fuzzy cluster analysis, additional features have been added to the program package. During preprocessing, pixel time-courses are examined with respect to auto-correlation and drifts as well as frequency and phase components. Only those pixels that pass the specific preprocessing criteria enter the clustering process and are iterated as described above. All other pixels are not simply rejected but are added before the last iteration in order to recover initially missed pixel time-courses. An additional feature of this fuzzy clustering algorithm is the so-called merging factor. It is a threshold for z -scores calculated between two clusters at the end of each iteration. If their mutual z -scores are below the merging factor, these clusters are combined [27]. Further, to test the clusters for significance, a resampling technique [8] or other methods may be applied.

Depending on technical details of the fMRI experiment performed, these preprocessing and merging features allow to enhance clustering performance in two ways: (a) the number of pixels clustered as well as the number of clusters is largely reduced, thus, cutting computation time, and (b) it is possible to “sensitize” the clustering procedure towards certain temporal features (e.g. if one would be interested in studying cardiac artifacts, a frequency range corresponding to the heartbeat can be chosen). With this implementation of fuzzy clustering temporal centroids or cluster centers (average time-courses per cluster) and spatial membership maps are obtained. All time-courses of a cluster are then correlated to the corresponding cluster centroid and a color-coded correlation coefficient map is overlaid to the image data. For more details see [46].

2.2. *Subjects and MR scanners*

Subjects examined in our studies are recruited either from the academic environment of the University of Vienna (studies III–V at 3 T) or University of Pennsylvania (study I at 4 T). None of them had known neurological disorders, and all gave written informed consent prior to the examination after extensive information on the nature of the experiment.

Measurements were performed at high-field either on a Medspec S 300 whole-body scanner (Bruker Medical, Ettlingen, Germany) operating at 3 T, or on a Signa Horizon (General Electric, Milwaukee, Wisconsin, USA) with a magnetic field strength of 4 T, both equipped with their manufacturers whole-body gradient system and the standard birdcage-type head coil for excitation and reception. To reduce motion artifacts, subjects’ heads were comfortably fixed with anatomically formed cushions and/or a strap around the forehead.

2.3. *Study I: Temporal patterns of physiological fluctuations and motion artifacts*

In this experiment, we tried to evaluate the performance of FCA to differentiate temporal patterns in fMRI time series data. We used a test object consisting of two components: a bottle of doped water representing the static part and a flexible tube wrapped around this bottle. Water was pumped through that tube leading to pulsatile flow. This setup was designed to simulate in vivo conditions where the brains rests within pulsating vasculature. We acquired 300 images of one slice with a repetition time TR of 200 ms and an echo time TE of 84 ms. In addition to demonstrate the potential of FCA to differentiate temporal patterns in vivo we analyzed a fMRI data set measured at 4 T where human faces showing different emotions were used as stimuli [44].

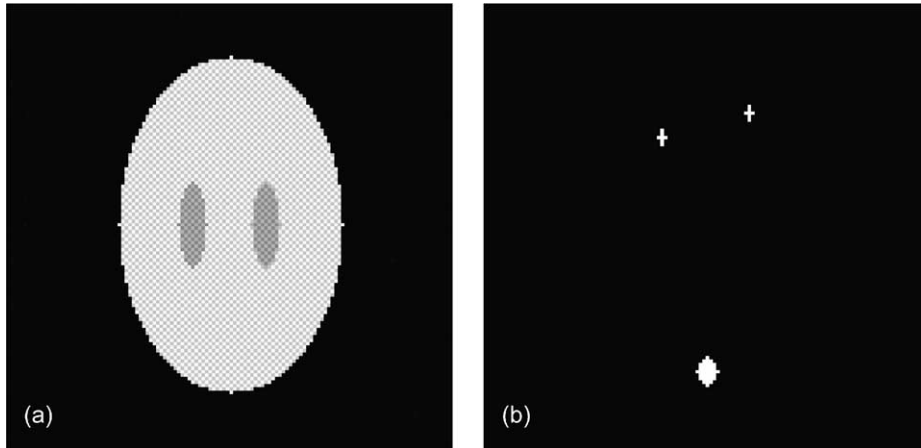


Fig. 1. The synthetic data set represents a single axial brain slice (matrix size 128×128), with a time invariant anatomy (a) over the 35 time points with signal variations at the location of three activation spots across the slice (b). The number of “activated” pixels in the three white spots is $N_{\text{act}} = 49$. The background “anatomy” consists of a checkered pattern with lower and higher signal intensity components, simulating gray and white matter with cerebro-spinal fluid filled ventricles, respectively.

2.4. Study II: Synthetic fMRI data (block design)

This study was performed to quantitatively test the sensitivity of relevant FCA parameters on clustering results. We used a synthetic fMRI data set calculated specifically to evaluate the performance of fMRI evaluation algorithms [2,9,15,31]. This data set represents a single axial brain slice (matrix size 128×128), with a time invariant anatomy over the 35 time points (see Fig. 1) with signal variations at the location of activated areas (i.e. three spots across the slice; block design: CECECEC (C: control, E: experimental task), five images each). The number of pixels in area A was $N_A = 35$ and in area B it was $N_B = 14$, thus, $N_{\text{act}} = 49$). The background “anatomy” consists of the following structures: a checkered pattern representing lower signal intensity (SI), $SI = 204$ ($N = 2268$) and higher signal intensity components, $SI = 241$ ($N = 2268$), simulating gray and white matter, respectively. Cerebro-spinal fluid filled ventricles are also represented by a checkered pattern with lower and higher intensity components, $SI = 156$ ($N = 145$) and $SI = 192$ ($N = 145$), respectively. Signal enhancement in activation areas A and B ranged from 4 to 10%. The data sets were corrupted by white noise (mean 3%), resulting in contrast-to-noise ratios (CNR) in the range of 1.33–3.33 between “non-activated brain” and “activated” regions A and B. In addition, a random baseline shift simulating thermal shifts in a temporal image series was introduced, not exceeding 1% of the baseline level. All together, at least ten different clusters may be obtained.

Receiver–operator characteristics analyses were performed according to [13]. ROC-curves were created for both FCA and CA by varying both membership threshold (MTH; for those clusters showing the expected temporal activation pattern) and correlation threshold (CTH) between 0.4 and 0.99 (step size of 0.005) and calculating the corresponding true-positive (TP) and false-positive (FP) fraction. Using this procedure the influence of the fuzzy index (FI;

varied between 1.0 and 1.4), initial number of clusters (INC; varied between 15 and 50), which is not known a priori and must be chosen in advance, and merging factor (M ; varied between 0 and 10) on the clustering performance was investigated.

2.5. Study III: *In vivo fMRI data of human motor cortex activity (block design)*

This study consisted of a block-design paradigm with three consecutive “off–on” periods and an additional baseline block at the end (10 images per block). During the “on” periods of 20 s subjects performed a finger-tapping task, paced by the acoustic pattern of the sequence. A three-dimensional set of T_1 -weighted images of the head, including exactly the same slices as the fMRI measurements, were obtained for anatomical details from every subject. To avoid gross motion artifacts subjects’ heads were comfortably fixed using a vacuum pillow and ear-pads. In order to compare FCA with a model-based analysis technique, we also used a standard cross-correlation method [3] with a box-car reference function shifted by three time points (i.e. 6 s) to account for delays in the haemodynamic response. In addition, we selected clusters from the first FCA step and performed a second analysis to separate high and low activation amplitudes [9,30].

2.6. Study IV: *Multi-echo spiral imaging of sequential finger tapping at 3 T (block design)*

Ten healthy young subjects were examined using a multiple echo, single-shot spiral imaging sequence implemented on the 3 T scanner [4]. Five slices covering the motor cortex were acquired at eight different echo times (echo time $TE = 5–180$ ms, echo spacing of 25 ms, repetition time $TR = 3$ s, spatial resolution = $4\text{ mm} \times 4\text{ mm} \times 4\text{ mm}$). One task period for functional imaging consisted of a right-hand self-paced finger to thumb movement performed during 30 s. Three task periods were each preceded by a resting period without a task. This block was followed by an additional resting period at the end resulting in a total of 70 time instances. For further details about the sequence design and image reconstruction refer to [4].

The first four time instances were excluded to assure equilibrium state images. All echo times instances were normalized to the first echo and integrated in a single data set with a total of 528 time instances, in this case “time” meaning a combination of time and echo time (refer to [5] for processing of multi-echo data). This procedure allows the clustering process to minimize the Euclidean distance between pixel time-courses including information on echo time dependence which is inherently influenced by physiological properties (e.g. blood volume, vessel geometry, blood–oxygen saturation). After the first clustering step, it is possible to further split the regions-of-interest (ROIs) from the first pass in several (sub-)clusters in a second step (see study III). A qualitative estimation of tissue blood volume was used to classify the resulting clusters.

2.7. Study V: *BOLD–EPI of mental rotation at 3 T (event-related)*

We examined seven young healthy male subjects and used a so-called event-related paradigm design, where single stimuli (items) are presented sequentially, rather than alternating blocks of stimuli with rest. Each task item consisted of two three-dimensional

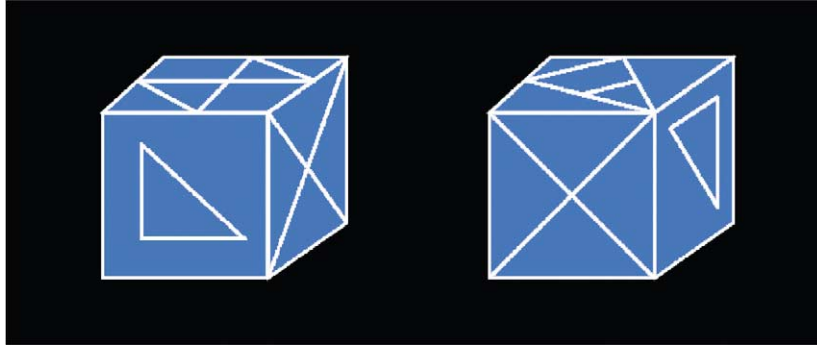


Fig. 2. Sample stimuli for study V. Subjects had to decide whether both cubes could be identical by viewing only three out of six sides of the three-dimensional cube. This task requires the “mental” rotation of one of the two cubes.

views of cubes [20] with simple geometric patterns on their sides (lines, triangle, arrows; see Fig. 2a). The subjects had to decide whether the two cubes could be identical, given the fact that every pattern occurs only once on each cube. This required the mental rotation of one cube into the orientation of the other. Items were presented through MR-compatible goggles (Resonance Technologies, USA), and subjects had a button panel on their right thigh for answering. Between item presentations the stimulus switched backed to a baseline image (Fig. 2b), consisting of the “shadows” of the two cubes, as well as a central cross for eye fixation to reduce motion artifacts.

Fifteen axial slices with a matrix size of 64×64 pixels were imaged every 1.5 s at a TE of 23 ms using a single-shot blipped gradient-recalled EPI sequence. The field-of-view (FOV) was 190 by 190 mm resulting in an in-plane resolution better than 3 mm. We acquired two runs of 15 min (600 image slabs) each. Prior to data analysis, fMRI data sets were realigned in two-dimensional using automated image registration (AIR) [51] to compensate for gross head motion effects.

Similar to study III we used a two-step FCA approach. The computation times were less than 2 min for both clustering steps in this study on a Pentium II 500 MHz PC running SuSE Linux. The cluster centers corresponding to the mental rotation paradigm are of much higher frequency than in the block-design stimulus of the previous study, i.e. closer to frequencies of physiology-related fluctuations (e.g. respiration). The two subsequent 15 min studies were analyzed separately. To improve FCA performance, we chose a frequency range close to the number of items presented per study in order to preselect pixel time-courses for cluster initialization.

3. Results

3.1. Study I: Temporal patterns of physiological and motion artifacts

Stability measurements on a test object consisting of a static part (i.e. a bottle of doped water) and dynamic structures (i.e. tubes with pulsating flow), analyzed by fuzzy

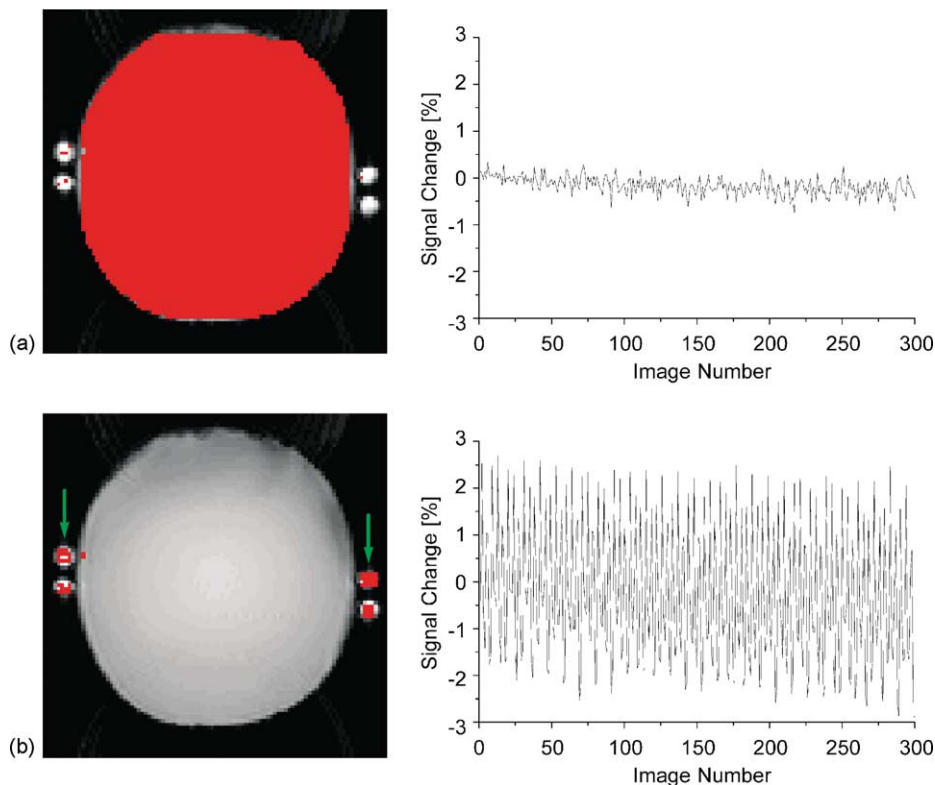


Fig. 3. Separation of pixel time-courses by fuzzy cluster analysis of test object data. Average time-courses (right) and corresponding membership maps (left) are shown, where pixels, which are cluster members, are overlaid on a standard grey-scale MR-image in red. (a) Cluster 1 displays the high signal stability within the static part of the test object, and (b) cluster 2 represents the pulsatile flow in the outer tubes (green arrows), the signal changes perfectly matching the pulsation frequency of the pump.

clustering, revealed the high stability and reproducibility of the hardware performance and the single-shot gradient-recalled echo-planar-imaging (EPI) sequence applied (rms intensity variations $\pm 0.1\%$ over 300 time points within the static part). Two clusters and their corresponding time-courses are shown in Fig. 3: (a) cluster 1 representing the static part and (b) cluster 2 consisting of pixels within the areas of pulsating flow (arrows). Note the perfect separation of static water (Fig. 3a) from pulsatile flow (Fig. 3b) and even the detection of static components in the tubes. The discrimination of slow and fast signal changes is of great importance in fMRI as it may help to separate brain activation patterns from physiological artifacts, e.g. respiration and cardiac action.

Apart from scanner-induced artifacts (e.g. image distortion due to very fast acquisition), gross head motion as well as physiological movements are a common nuisance in fMRI data sets and decrease sensitivity of fMRI results. Fig. 4 shows examples for head motion: in-plane motion (red) and through-plane motion (green) from the same data set.

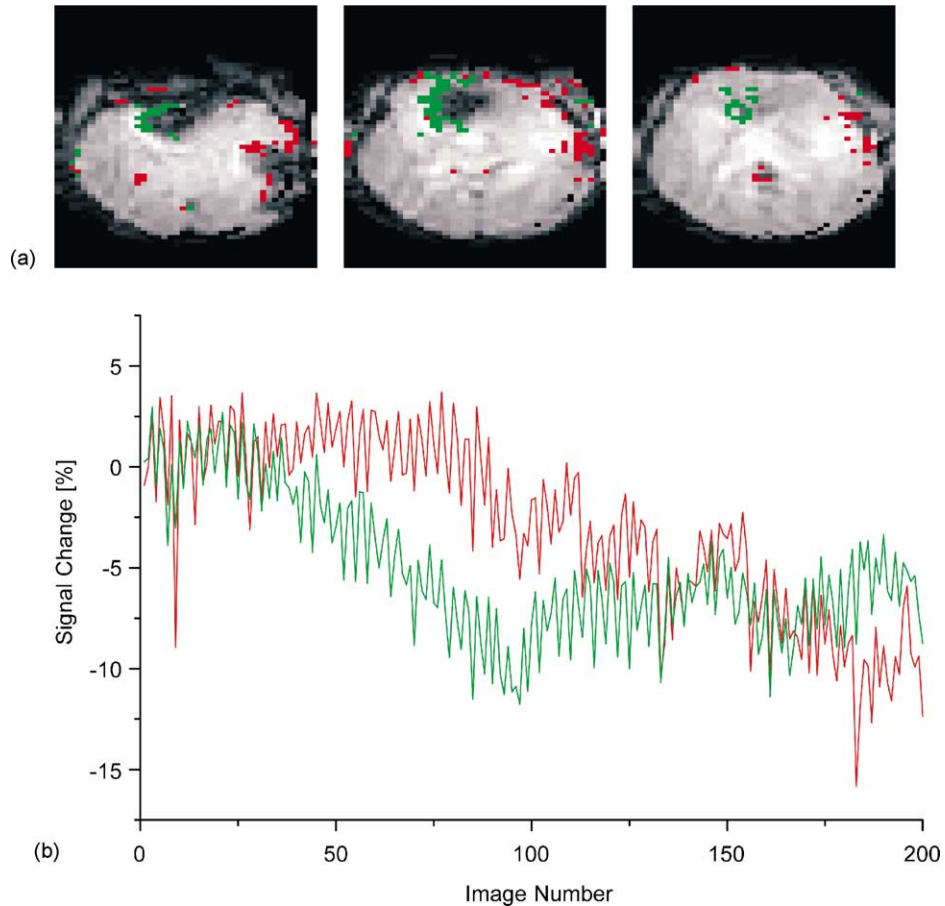


Fig. 4. Demonstration of artifacts caused by in-plane (red) and trough-plane (green) motion in BOLD-EPI at 4 T. Signal changes are enhanced by susceptibility differences near tissue-CSF or tissue-air interfaces (a). Note also the characteristic signal intensity drift (b) and pixel distribution.

Also note the strong susceptibility-based artifact (dark region in the frontal part of the brain) from the distant sinuses.

3.2. Study II: Synthetic fMRI data

For $\text{CNR} > 1.66$, the ROC curves were almost identical for FCA and CA and showed no false-positives (FP) for any threshold applied. Differences between the two methods can be seen with $\text{CNR} \leq 1.66$ (Figs. 5 and 6). ROC curves for different initial number of clusters ($\text{INC} = 15, 25, 50$) and merging factors ($M = 0, 1, 2, 4, 6, 8-10$) are displayed in Fig. 5. It can be seen that the overall performance clearly increases with higher INC, almost independent of M . If INC is chosen too low, i.e. ≤ 15 in our case, results are getting less optimal as too many FP are assigned to the activation cluster. However, due to the short

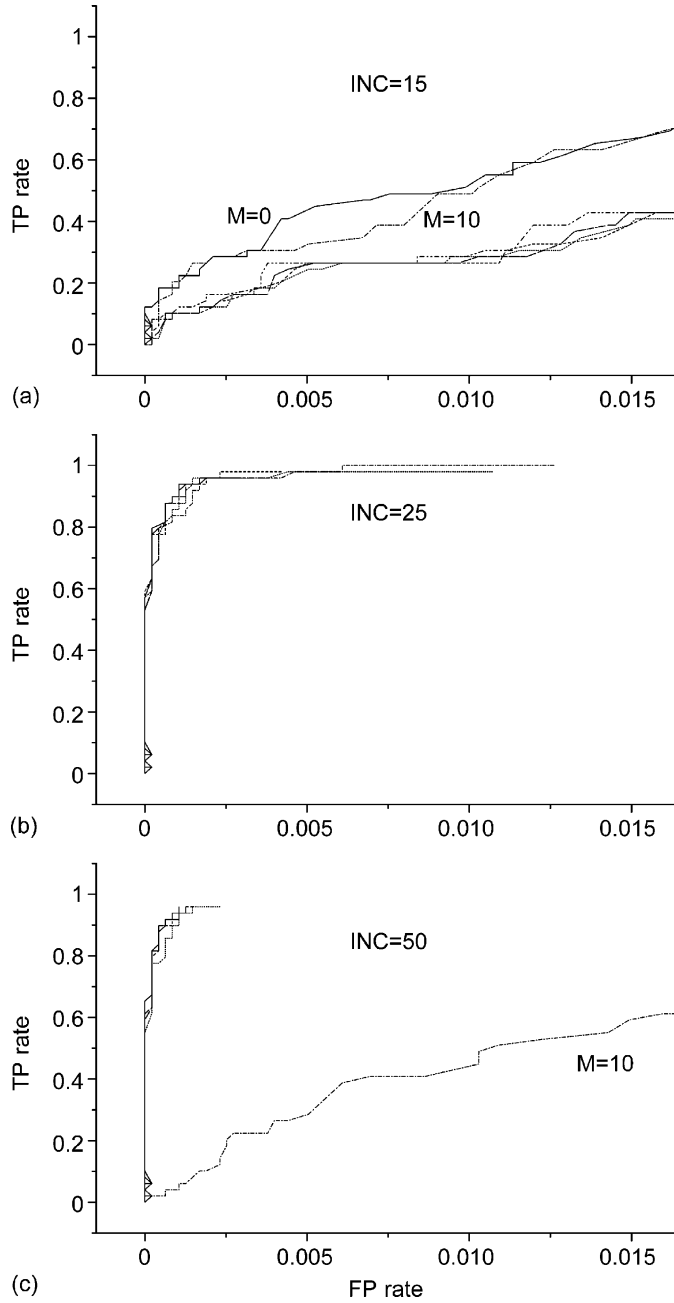


Fig. 5. ROC analysis with image CNR ≤ 1.66 for different initial number of clusters. INC = 15 is shown in (a), INC = 25 in (b), INC = 50 in (c). Merging factors were varied between 0 (solid line) and 10 (dashed-dotted line) for each INC. It can be seen that the overall performance clearly increases with higher INC, almost independent of M . FCA performs best with INC = 50 and $M = 1$.

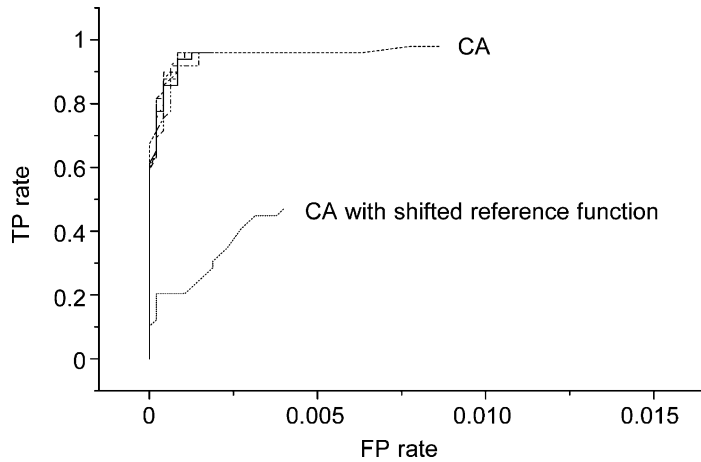


Fig. 6. ROC curves for FCA with $INC = 50$ and $M = 1$ varying the fuzzy index FI from 1.0 (i.e. crisp clustering) to 1.4 (upper curves). The plot reveals that CA (dashed line) and FCA with a fuzzy index of 1.1 (solid line) perform equally well. Changing FI to a lower (1.0) or higher value (up to 1.4) still shows a good stability of FCA. However, in contrast to FCA, CA performance drops rapidly when the reference time-course is shifted by one time instant only (dotted line).

computation times for this algorithm (a few seconds only for each run) there is no practical limitation to use large INC , even for very large data sets. No overall rule can be given for M , but as long as the INC is sufficiently large the influence of M is very small, although excessive merging ($M = 10$) can cause a significant increase in FP (cf. Fig. 5c).

From the results above it can be seen that FCA with $INC = 50$ and $M = 1$ performs very well. Using these parameters the analysis was repeated varying the fuzzy index FI from 1.0 (i.e. crisp clustering) to 1.4. The plots in Fig. 6 show that CA and FCA with a fuzzy index of 1.1 perform equally well. Changing FI to a lower (1.0) or higher value (up to 1.4) still shows a good stability of FCA, however, achieving slightly less optimal activation separation. For this data set, the exact time-course is known and used for CA. For in vivo data sets the time-course varies from subject to subject even for block-design paradigms due to variations of the haemodynamic response (e.g. onset, delay, ...). To account for such a haemodynamic delay, which can range from 4 to 10s [22], time-course shifting is regularly applied in correlation analysis of fMRI data. If the estimate for this delay is wrong and the reference function is shifted too much, CA performance drops rapidly as shown by the dotted ROC curve in Fig. 6 where the reference time-course shifted by one time instant only.

3.3. Study III: Motor cortex activation

We found significant activation in all subjects, located in areas that represent parts of the human sensorimotor system, i.e. contralateral primary motor region and supplementary motor areas (SMA), as well as ipsilateral activation along the central sulcus. Fig. 7 shows typical activation maps in a single subject: (a) FCA and (b) CA results. The corresponding time-courses are shown in Fig. 7c. Through the Euclidean distance as

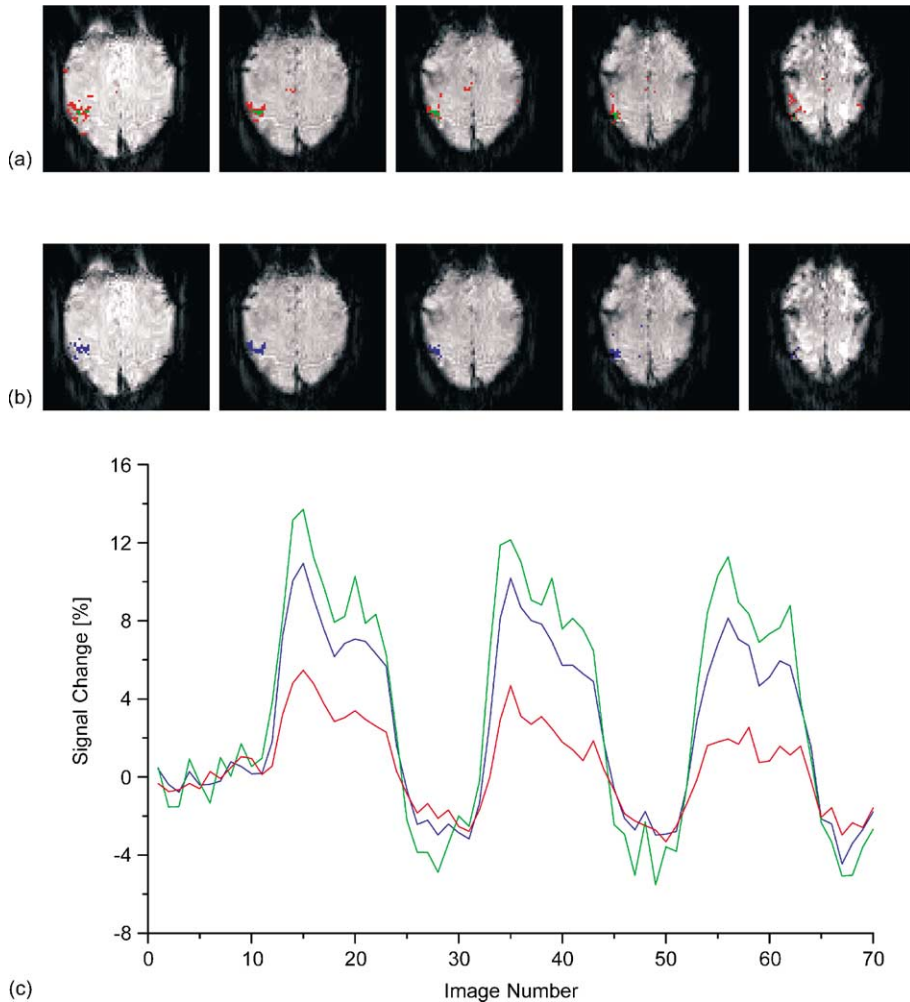


Fig. 7. Membership maps (a) and corresponding signal time-courses (c) from a representative subject (5 different slices out of 15) of study III, showing large vessel contributions (green) and microvasculature related brain activation (red) in the human motor cortex. For comparison, results of a standard correlation analysis of the same data set are given in blue (b). Note the strong bias towards high-amplitude signal changes (shown in c) which does not allow any differentiation between macro- and microvessels (b) and hampers detection of activation in SMA.

a similarity measure in FCA, it was possible to separate different activation amplitudes: low activation amplitude cluster (red pixels, signal enhancement approximately 4%) and high amplitude cluster (green pixels, approximately 10%). From the localization of activated pixel in the slices shown it can be seen that the low-amplitude pixels represent “true” cortical activation in very small veins, whereas high amplitudes correspond to larger draining veins distant from the site of neuronal activity. For comparison,

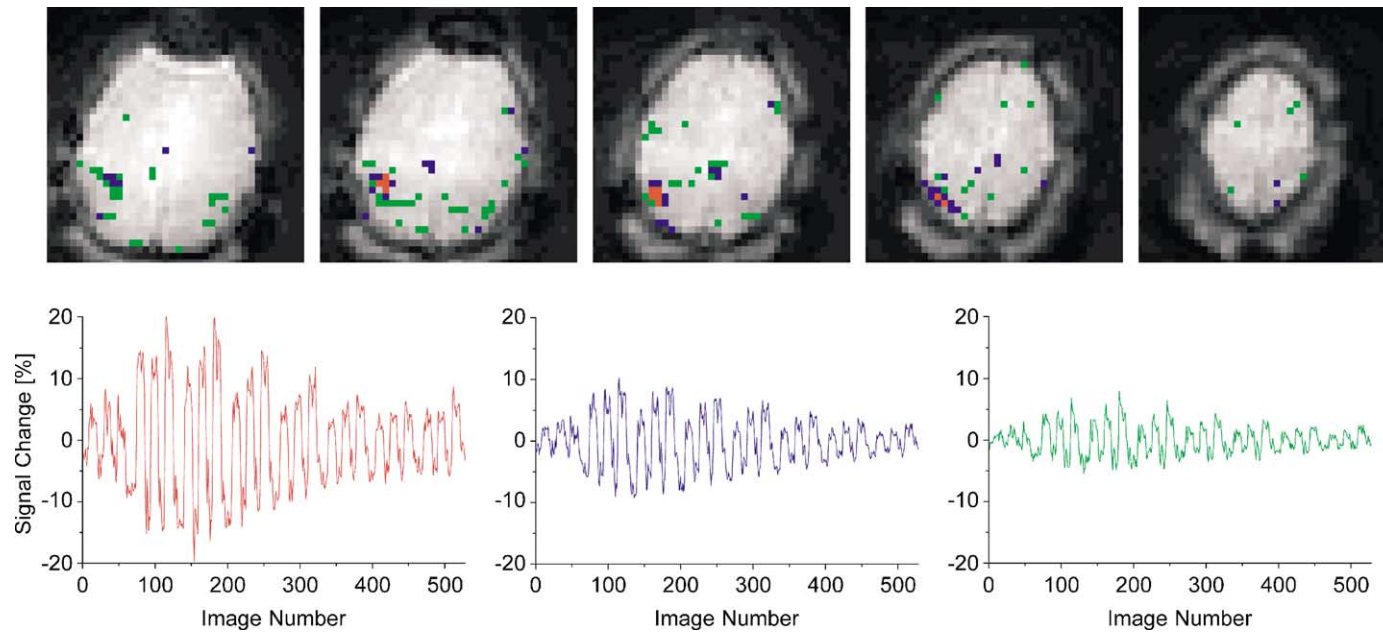


Fig. 8. Multi-echo analysis results (study IV). Top: the activated pixels are shown in colors corresponding to the clusters representing higher (red) and lower (blue, green) blood volume fractions. Bottom: the time-courses (cluster centers) corresponding to these clusters are shown. Maximum signal enhancement (%) reflects maximum sensitivity, however, not necessarily towards microvasculature.

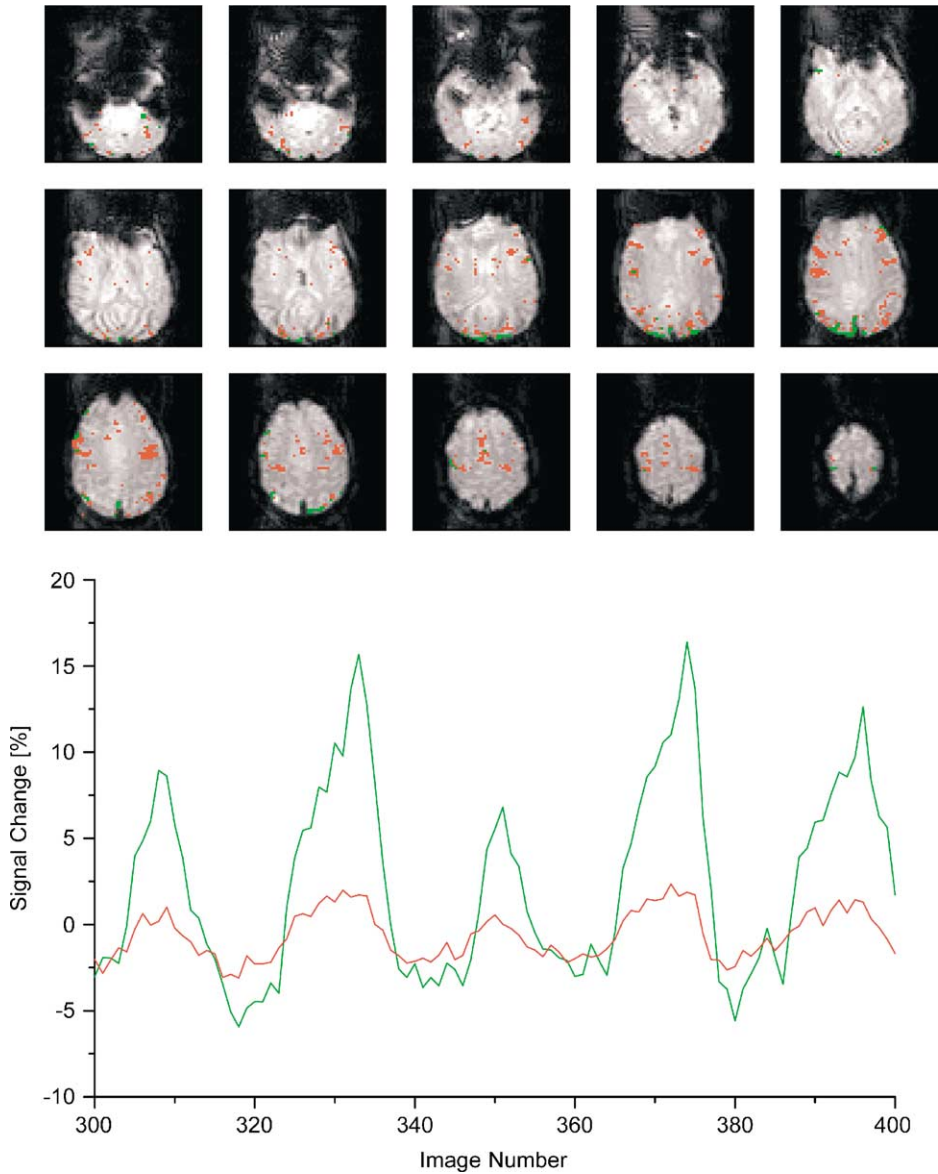


Fig. 9. fMRI of mental rotation (study V): activation maps for a single subject and the corresponding time-courses (only 100 time points out of 600 are displayed) of the high-amplitude (green) and the low-amplitude cluster (red). The five peaks reflect five subsequent mental rotation tasks (different pair of cubes). Localization of green voxels suggest draining veins, while red voxels indicate expected spatio-temporal processing.

model-based cross-correlation analysis results in a mixture of low- and high-amplitude pixels (blue) and, therefore, activation maps which do not allow differentiation (Fig. 7b).

3.4. Study IV: Multi-echo spiral imaging of sequential finger tapping at 3 T

The resulting images using the evaluation method described in Section 2 are presented in Fig. 8, which shows the extracted three activation clusters of a single subject color coded red, blue, and green with their corresponding cluster centers. Consistent activation was found in the primary motor cortex (M1) and supplementary motor area (SMA) for all subjects. The signal oscillation is caused by alternation of deactivation and activation periods (three per echo time) during all echo times ($8\times$) and can be seen easily (24 peaks resulting). The amplitude as well as the shape of the curves differ from cluster to cluster. In Fig. 8 (top), all five slices measured are displayed with the three clusters colored accordingly (red, blue, green). It can be seen that the activated pixels of the red cluster are found in the center of the activated area, that the second cluster is enclosing the first, and that the third is distributed more diffuse over the brain. The time-course characteristics of the first (Fig. 8, red) cluster can be interpreted with a high blood volume fraction within a voxel which indicates large vessel contributions, the other (blue and green) cluster centers exhibit a dependence which indicate a much smaller blood volume fraction and might, therefore, be interpreted as smaller vessels or microvasculature.

3.5. Study V: BOLD–EPI of mental rotation at 3 T

FCA was able to extract activation patterns in all subjects, without exact information about the stimulus paradigm. Fig. 9 shows the resulting clusters from the second clustering step for a single subject. Note that for clarity only 100 time points (out of 600) are plotted in Fig. 9 (bottom). The five peaks correspond to five successive but different stimuli. Cluster 1 (green) consists of pixels with very high activation amplitudes of 10–15%. From the activation maps in Fig. 9 (top) it can be concluded that the corresponding pixels represent larger veins, distant from the site of neuronal activity. In contrast, the red pixels of cluster 2 are located in areas known to be essential for visuo-spatial processing like the parietal cortex, premotor areas, dorso-lateral prefrontal cortex, as well as supplementary motor areas.

4. Discussion

In this paper we attempt to evaluate the performance of FCA in terms of: (a) the ability to differentiate between different signal time-courses (study I), (b) the influence of clustering parameter selection on FCA results in terms of ROC using synthetic data (study II), (c) a comparison of FCA to a widely used model-based correlation analysis approach both using synthetic (study II) and in vivo fMRI data (study III), (d) the differentiation of vascular signal sources based on either signal enhancement (studies III–V) or echo-time dependence (study IV). The data sets examined also cover the two most often used paradigm designs: blocked (studies II–IV) and event-related stimulus presentation (study V).

From the results of study I, it can be seen that FCA performed almost perfect in separating static from pulsating pixel time-courses in the test object data (Fig. 1). Similar, motion artifacts in fMRI data from the human head are easily detected. The corresponding time-courses are typical for such artifacts and easily identified based on both the cluster centroids and the distribution of the corresponding pixels. A more problematic variant is stimulus-correlated motion, which shows the same temporal behavior as functional activation and, therefore, may not be separated that easily. fMRI data sets are often contaminated by a variety of artifacts, ranging from low-frequency fluctuation (“functional connectivity”, scanner drifts, head motion) to respiration-related signal changes, and up to high frequency pulsation due to cardiac action. All of these sources of artifacts need to be considered in fMRI analysis, especially if a brain region is examined that is particularly susceptible (e.g. the brain stem). In this way, FCA can be used to examine the performance of methods for motion correction or techniques for the reduction of physiological fluctuations [12–30].

Using a synthetic fMRI data set enables a quantitative comparison between different statistical and exploratory post-processing methods. As shown from the analysis of the synthetic fMRI data, FCA performs robust provided that INC is not too small (≥ 20) and moderate merging is applied. ROC analysis from FCA results with different levels of fuzziness also shows that the choice of FI does not influence FCA performance significantly if it is kept within reasonable limits. For the synthetic data used a FI of 1.1 is optimal in terms of ROC, but it should be kept in mind that the tests were performed with simulated single-slice fMRI data using a block design and a random noise distribution. This setup would definitely favor standard correlation analysis. For in vivo fMRI data, however, with different sources of noise and expected and unexpected activation patterns, FCA has advantages over model-based analysis approaches like CA, as a major problem in fMRI analysis using model-based methods is the construction of a reference function. This function should represent the haemodynamic response, i.e. the time-course of activated pixels. Even in block-design studies where long (compared to the image repetition time) stimulation periods are used it is not always possible to accurately predict the haemodynamic response delay [22]. If this delay is estimated too short or too long, in general all model-based analysis methods will perform sub-optimal. We showed (see Fig. 6) that even slight errors in estimating the haemodynamic response (i.e. shifting by one time point only) can lead to a severe decrease of CA performance. Data-driven methods like FCA do not require the expected response delay as an input and, therefore, are not biased towards short or long haemodynamic delays.

The comparison of CA and FCA applied to in vivo fMRI data (study III; finger tapping, block design) also underlines the potential of FCA as the study design actually would favor CA. It has also been shown that multivariate statistical approaches like principal component analysis are inherently limited and biased towards large signal changes (e.g. motion or large vessels; see, e.g. [6]). In comparison to other model independent approaches like self-organizing maps [16,34] or independent component analysis [29], FCA as implemented in EvIdentTM is superior in terms of speed (i.e. below 1 min versus hours) and/or data reduction, both important factors in (clinical) fMRI data analysis. Nevertheless, to validate neurophysiological models of brain activation, established statistical procedures should be used, potentially using improved hypotheses extracted via exploratory data processing [46].

With more complex tasks, in particular single trial designs, FCA may be superior over model dependent approaches. However, whether (significant) activation in the human brain is detected may also depend on factors like preprocessing of the data sets (e.g. motion correction and normalization), the actual algorithm (i.e. proximity measure, details of the implementation and parameter settings), the reference function employed (if required), the (varying) individual haemodynamic delay, the threshold(s) applied, and the (inherent) assumptions concerning the noise distribution during both, resting and activation periods.

The potential of FCA in exploring fMRI data sets can also be demonstrated in the analysis of complex multi-echo data (study IV). Here even more (at first unknown) features of the haemodynamic response can be investigated, e.g. the changes of signal amplitude versus echo time. These changes are dependent on a number of vascular properties such as vessel orientation and size, most of them unknown as they differ significantly between subjects and brain regions. FCA enables to obtain time-courses that are characteristic for certain vascular properties. The results of this evaluation procedure may then provide the basis for quantitative biophysical modeling where vascular and tissue properties must be known and included [24,25,53]. Subsequently, from both the signal enhancement during activation and echo time dependence it is possible to differentiate between activation in small venules and larger draining veins. This strategy for characterization of activation based on the behavior of different vessel environment on the acquisition parameter TE might be very helpful for clinical applications of fMRI, e.g. distinct localization in presurgical planning [10].

Finally, an application of FCA in cognitive fMRI has been presented (study V). Again, the main advantage of a data-driven analysis is that there is no need for a particular reference function. Generation of reference functions for model-based analysis methods is not straight-forward, especially in cognitive tasks where verification of cognitive activity is hardly possible. This study used long acquisition periods (2×15 min), stimuli with rather long processing times (up to 60 s) as well as a large number of stimuli (up to 60 for both runs). Therefore, it is likely that not only drifts and motion artifacts will affect the data but also “psychological instabilities” like decreased attention as it cannot be expected that subject cooperation is constant throughout the scanning. There may possibly be some stimuli that are not mentally rotated by the subject as desired but rather guessed. Therefore, fMRI signal from brain regions which are truly involved in mental rotation might not be enhanced during every single stimulus presentation. Consequently, a reference function derived by simply convolving the stimulus presentation time-course with a “typical” haemodynamic response function might not be adequate, decreases sensitivity, and may lead to sub-optimal fMRI results [22]. Additionally, FCA with the Euclidean distance as similarity measure allows the separation of different activation amplitudes and leads to increased specificity. Therefore, EDA seem to be ideal for analyzing event-related cognitive fMRI studies.

5. Conclusion

A novel application of fuzzy logic in functional MRI has been introduced recently which may serve as a useful analysis tool in neuroscience and medical imaging. An EDA method

like FCA can serve as a very powerful data mining and first-pass data analysis tool in fMRI and provides information unavailable to standard evaluation methods that inherently require prior knowledge. The new information obtained with this data-driven approach can help to identify technical or physiological artifacts and may also help to improve the fMRI technique. In this paper, we have demonstrated the potential of FCA for exploratory analysis of both synthetic and in vivo fMRI data. FCA performs at least equal in reproducing the searched activation (i.e. TPs) compared to correlation analysis in cases of properly known stimulus response functions. This may improve the answer to the most commonly posed questions about brain activation: where did it occur (shown by the cluster membership map) and what are the temporal characteristics (depicted by the cluster centroid). As fuzzy cluster analysis is a paradigm independent approach for fMRI data analysis, FCA is able to identify anticipated as well as unexpected haemodynamic responses and artifact-related temporal patterns. The signal processing strategy used in FCA helps to extract the full amount of information without distorting model bias. Data presented here were restricted to oxygenation-contrast fMRI only, however, other potent MR applications may include dynamic perfusion imaging [32] or classification of spectra [37,38–52].

Acknowledgements

This study was financially supported by the Jubiläumsfonds der Österreichischen Nationalbank (P7174 and P8184). We gratefully acknowledge stimulating discussions with R. Baumgartner and R. Somorjai (Winnipeg, Canada).

References

- [1] Alexander ME, Baumgartner R, Windischberger C, Moser E, Somorjai RL. Wavelet domain de-noising of time-courses in MR image sequences. *Magn Reson Imag* 2000;18:1129–34.
- [2] Backfrieder W, Baumgartner R, Samal M, Moser E, Bergmann H. Quantification of intensity variations in functional MR images using rotated principal components. *Phys Med Biol* 1996;41:1425–38.
- [3] Bandettini PA, Jesmanowicz A, Wong EC, Hyde JS. Processing strategies for time-course data sets in functional MRI of the human brain. *Magn Reson Med* 1993;30:161–73.
- [4] Barth M, Metzler A, Klarhofer M, Roll S, Moser E, Leibfritz D. Functional MRI of the human motor cortex using single-shot, multiple gradient-echo spiral imaging. *Magn Reson Imag* 1999;17:1239–43.
- [5] Barth M, Reichenbach JR, Venkatesan R, Moser E, Haacke EM. High-resolution, multiple gradient-echo functional MRI at 1.5 T. *Magn Reson Imag* 1999;17:321–9.
- [6] Baumgartner R, Ryner L, Richter W, Summers R, Jarmasz M, Somorjai R. Comparison of two exploratory data analysis methods for fMRI: fuzzy clustering vs. principal component analysis. *Magn Reson Imag* 2000;18:89–94.
- [7] Baumgartner R, Scarth G, Teichtmeister C, Somorjai R, Moser E. Fuzzy clustering of gradient-echo functional MRI in the human visual cortex. Part I. Reproducibility. *J Magn Reson Imag* 1997;7:1094–101.
- [8] Baumgartner R, Somorjai R, Summers R, Richter W, Ryner L, Jarmasz M. Resampling as a cluster validation technique in fMRI. *J Magn Reson Imag* 2000;11:228–31.
- [9] Baumgartner R, Windischberger C, Moser E. Quantification in functional magnetic resonance imaging: fuzzy clustering vs. correlation analysis. *Magn Reson Imag* 1998;16:115–25.

- [10] Beisteiner R, Lanzenberger R, Novak K, Edward V, Windischberger C, Erdler M, et al. Improvement of presurgical patient evaluation by generation of functional magnetic resonance risk maps. *Neurosci Lett* 2000;290:13–6.
- [11] Bezdek JC, Ehrlich R, Full W. FCM: the fuzzy C-means algorithm. *Comp Geosci* 1984;10:191–203.
- [12] Biswal B, DeYoe AE, Hyde JS. Reduction of physiological fluctuations in fMRI using digital filters. *Magn Reson Med* 1996;35:107–13.
- [13] Constable RT, Skudlarski P, Gore JC. An ROC approach for evaluating functional brain MR imaging and postprocessing protocols. *Magn Reson Med* 1995;34:57–64.
- [14] Ding X, Tkach J, Ruggieri T, Masaryk P. Analysis of time-course functional MRI data with clustering method without use of reference signal. *Proc Soc Magn Reson* 1994;630.
- [15] Filzmoser P, Baumgartner R, Moser E. A hierarchical clustering method for analyzing functional MR images. *Magn Reson Imag* 1999;17:817–26.
- [16] Fischer H, Hennig J. Neural network-based analysis of MR time series. *Magn Reson Med* 1999;41:124–31.
- [17] Friston K. Imaging cognitive anatomy. *Trends Cogn Neurosci* 1997;1:21–7.
- [18] Friston K, Jezzard P, Turner R. Functional MRI of human brain activation at high spatial resolution. *Hum Brain Mapp* 1994;2:69–78.
- [19] Gati JS, Menon RS, Ugurbil K, Rutt BK. Experimental determination of the BOLD field strength dependence in vessels and tissue. *Magn Reson Med* 1997;38:296–302.
- [20] Gittler G. *Dreidimensionaler Würfeltest (3DW)*, Weinheim; 1990.
- [21] Golay X, Kollias S, Stoll G, Meier D, Valavanis A, Boesiger P. A new correlation-based fuzzy logic clustering algorithm for fMRI. *Magn Reson Med* 1998;40:249–60.
- [22] Goutte C, Hansen LK, Liptrot MG, Rostrup E. Feature-space clustering for fMRI meta-analysis. *Hum Brain Mapp* 2001;13:165–83.
- [23] Goutte C, Toft P, Rostrup E, Nielsen F, Hansen LK. On clustering fMRI time series. *NeuroImage* 1999;9:298–310.
- [24] Haacke EM, Lai S, Reichenbach J, Hoogenraad FG. In: Pavone P, Rossi P, editors. *Syllabus functional MRI*. Berlin: Springer; 1995. p. 62–5.
- [25] Hoogenraad FG, Pouwels PJ, Hofman MB, Reichenbach JR, Sprenger M, Haacke EM. Quantitative differentiation between BOLD models in fMRI. *Magn Reson Med* 2001;45:233–46.
- [26] Hu X, Le TH, Parrish T, Erhard P. Retrospective estimation and correction of physiological fluctuation in functional MRI. *Magn Reson Med* 1995;34:201–12.
- [27] Jarmasz M, Somorjai R. Time to join! Cluster-merging in unsupervised fuzzy clustering of functional MRI data. *Proc Int Soc Magn Reson Med* 1998;1:206.
- [28] Kwong KK. Functional magnetic resonance imaging with echo planar imaging. *Magn Reson Q* 1995;11:1–20.
- [29] McKeown MJ, Makeig S, Brown GG, Jung TP, Kindermann SS, Bell AJ, et al. Analysis of fMRI data by blind separation into independent spatial components. *Hum Brain Mapp* 1998;6:160–88.
- [30] Moser E, Baumgartner R, Barth M, Windischberger C. Explorative signal processing in functional MRI. *Int J Imag Syst Tech* 1999;10:166–76.
- [31] Moser E, Diemling M, Baumgartner R. Fuzzy clustering of gradient-echo functional MRI in the human visual cortex. Part II. Quantification. *J Magn Reson Imag* 1997;7:1102–8.
- [32] Moser E, Jungbauer P, Gharabaghi M, Windischberger C, Lang W. Fuzzy clustering of dynamic susceptibility contrast MRI at 3 T. *NeuroImage* 1999;9:S80.
- [33] Moser E, Windischberger C. Separation of physiological motion artifacts in single-shot EPI to improve reproducibility for functional MRI studies. *Proc Int Soc Magn Reson Med* 1998;1:133.
- [34] Ngan SC, Hu X. Analysis of functional magnetic resonance imaging data using self-organizing mapping with spatial connectivity. *Magn Reson Med* 1999;41:939–46.
- [35] Ogawa S, Lee TM. Magnetic resonance imaging of blood vessels at high fields: in vivo and in vitro measurements and image simulation. *Magn Reson Med* 1990;16:9–18.
- [36] Ogawa S, Menon RS, Tank DW, Kim SG, Merkle H, Ellermann JM, et al. Functional brain mapping by blood oxygenation level-dependent contrast magnetic resonance imaging. A comparison of signal characteristics with a biophysical model. *Biophys J* 1993;64:803–12.

- [37] Pizzi N, Choo LP, Mansfield J, Jackson M, Halliday WC, Mantsch HH, et al. Neural network classification of infrared spectra of control and Alzheimer's diseased tissue. *Artif Intell Med* 1995;7:67–79.
- [38] Pizzi NJ. Fuzzy pre-processing of gold standards as applied to biomedical spectra classification. *Artif Intell Med* 1999;16:171–82.
- [39] Purdon PL, Weisskoff RM. Effect of temporal autocorrelation due to physiological noise and stimulus paradigm on voxel-level false-positive rates in fMRI. *Hum Brain Mapp* 1998;6:239–49.
- [40] Raz J, Turetzky B. Wavelet ANOVA and fMRI. *Proc SPIE Wavelet Appl Signal Imag Process* 1999.
- [41] Richter W. High temporal resolution functional magnetic resonance imaging at very-high-field. *Top Magn Reson Imag* 1999;10:51–62.
- [42] Ruttimann UE, Unser M, Rawlings RR, Rio D, Ramsey NF, Mattay VS, et al. Statistical analysis of functional MRI data in the wavelet domain. *IEEE Trans Med Imag* 1998;17:142–54.
- [43] Scarth G, McIntyre B, Wowk R, Somorjai R. Detection of novelty in functional images using fuzzy clustering. *Proc Soc Magn Reson Eur Soc Magn Reson Med Biol* 1995;238.
- [44] Schneider F, Gur RC, Gur RE, Muenz LR. Standardized mood induction with happy and sad facial expressions. *Psychiatr Res* 1994;51:19–31.
- [45] Somorjai R, Jarmasz M. Exploratory data analysis of fMR images: philosophy, strategies, tools, and implementation. *Proc Int Soc Magn Res Med* 1999;1714.
- [46] Somorjai R, Jarmasz M, Baumgartner R. A Fast, Two-stage strategy for the exploratory analysis of functional MRI data by temporal fuzzy clustering. *Proc Comp Intell Methods Appl (CIMA 2001)*, Paper: 1733-042.
- [47] Somorjai RL, Nikulin AE, Pizzi N, Jackson D, Scarth G, Dolenko B, et al. Computerized consensus diagnosis: a classification strategy for the robust analysis of MR spectra. I. Application to ¹H spectra of thyroid neoplasms. *Magn Reson Med* 1995;33:257–63.
- [48] Sychra JJ, Bandettini PA, Bhattacharya N, Lin Q. Synthetic images by subspace transforms. I. Principal components images and related filters. *Med Phys* 1994;21:193–201.
- [49] Thulborn KR. Clinical rationale for very-high-field (3 T) functional magnetic resonance imaging. *Top Magn Reson Imag* 1999;10:37–50.
- [50] Windischberger C, Beisteiner R, Cunnington R, Edward V, Kaindl T, Erdler M, et al. Fuzzy cluster analysis of single-event functional MRI in the human motor cortex. *Proc Exp NMR Conf* 1999;253.
- [51] Woods RP, Grafton ST, Watson JD, Sicotte NL, Mazziotta JC. Automated image registration. II. Intersubject validation of linear and nonlinear models. *J Comput Assist Tomogr* 1998;22:153–65.
- [52] Xu J, Weber PL, Borer PN. Computer-assisted assignment of peptides with non-standard amino acids. *J Biomol NMR* 1995;5:183–92.
- [53] Yablonskiy DA, Haacke EM. Theory of NMR signal behavior in magnetically inhomogeneous tissues: the static dephasing regime. *Magn Reson Med* 1994;32:749–63.
- [54] Zaroubi S, Goelman G. Complex denoising of MR data via wavelet analysis: application for functional MRI. *Magn Reson Imag* 2000;18:59–68.